Biochemistry

pubs.acs.org/biochemistry Article

# Finding Ways to Relax: A Revisionistic Analysis of the Chemistry of *E. coli* GTP Cyclohydrolase II

Madison M. Smith, Brett A. Beaupre, Dariush C. Fourozesh, Kathleen M. Meneely, Audrey L. Lamb, and Graham R. Moran*

Cite This: *Biochemistry* 2021, 60, 3027−3039 Read Online

ACCESS | Metrics & More | Article Recommendations | Supporting Information

**ABSTRACT:** Guanosine triphosphate (GTP) cyclohydrolase II (RibA) is one of three enzymes that hydrolytically cleave the C8−N9 bond of the GTP guanine. RibA also catalyzes a subsequent hydrolytic attack at the base liberating formate and in addition cleaves the $\alpha-\beta$ phosphodiester bond of the triphosphate to form pyrophosphate (PPi). These hydrolytic reactions are promoted by tandem active-site metal ions, zinc and magnesium, that respectively function at the GTP guanine and triphosphate moieties. The RibA reaction is part of riboflavin biosynthesis and forms 2,5-diamino-6-$\beta$-pyrimidinone 5′-phosphate, an exocyclic pyrimidine nucleotide that ultimately forms the pyrimidine ring of the isoalloxazine of riboflavin. The stoichiometry of the RibA reaction was defined in the study that first identified this activity in *Escherichia coli* (Foor, F., Brown, G. M. *J. Biol. Chem.*, **1975**, *250*, 9, 3545−3551) and has not been quantitatively evaluated in subsequent works. Using primarily transient state approaches we examined the interaction of RibA from *E. coli* with the GTP, inosine triphosphate, and PPi. Our data indicate that PPi is a slow substrate for RibA that is cleaved to form two phosphate ions (Pi). A combination of real-time enzymatically coupled Pi reporter assays and end-point $^{31}$P NMR revealed that Pi is formed at a catalytically relevant rate in the native reaction of RibA with GTP, redefining the reaction stoichiometry. Furthermore, our data indicate that both PPi and GTP stimulate conformational changes prior to hydrolytic chemistry, and we conclude that the cleavage of PPi bound as a substrate or an intermediate state results in conformational relaxation.

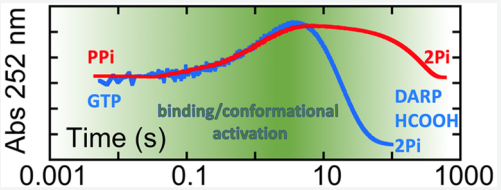




## INTRODUCTION

Guanosine triphosphate (GTP) cyclohydrolase II (RibA) is a dimeric enzyme that catalyzes one of the two committed steps in the convergent biosynthetic pathway that forms riboflavin. The reaction is reported to convert the substrate GTP into three products formate, pyrophosphate (PPi), and 2,5-diamino-6-$\beta$-pyrimidinone 5′-phosphate (DARP)[1−7] (Scheme 1). RibA requires two divalent metal ions, zinc and magnesium, for activity and both metal ions are believed to participate by a coordination of water molecules to promote hydrolytic chemistry. The structure of RibA solved with the substrate analogue GMPcPP, which has a carbon in place of the oxygen between the $\alpha$ and $\beta$ phospho groups, indicated that the GTP substrate is oriented such that the Zn is localized near the C8 of the purine and the Mg is proximal to the $\alpha,\beta$-phosphodiester linkage of the triphosphate moiety.[3]

RibA belongs to a class of three cyclohydrolase proteins that are named for the order in which they were discovered (I to III).[1,8,9] Each of these proteins catalyzes the hydrolytic cleavage of the GTP purine C8−N9 bond but forms structurally distinct products.[7] GTP cyclohydrolase I catalyzes a ring expansion to form dihydroneopterin triphosphate, cleaving the purine C8 as formate.[8] GTP cyclohydrolase III catalyzes the hydrolytic cleavage of the C8−N9 bond to form 2-amino-5-formylamino-6-$\beta$-pyrimidinone 5′-phosphate (FAPy) and the hydrolysis of both phosphodiester linkages to form two molecules of phosphate (Pi).[9] It has reasonably been inferred that the chemistry catalyzed by RibA is comprised only of hydrolytic steps; however, the order and mechanism with which these individual reactions occur has not been established. The reason for this is that RibA has proven to have a relatively slow initial step such that, observationally, GTP is converted to $\beta$-DARP in a single phase without accumulated intermediates.[6] As such, hypothetical chemical mechanisms for the chemistry have been proposed but are largely unsupported by evidence. One recurrent proposal has been that an active-site nucleophile is required to displace PPi from GTP and that this reaction tethers to the enzyme the GMP produced.[2,3,5,6,10] This proposal arose from the observation that GMP is not a substrate for RibA. Possibly the most direct evidence of a mechanism has come from Schramek and co-workers, who formed FAPy triphosphate from a variant form of GTP cyclohydrolase I and then demonstrated its conversion to DARP by RibA, indicating that FAPy is a potential intermediate state for RibA.[6,11]

**Received:** July 28, 2021
**Revised:** September 13, 2021
**Published:** September 27, 2021





https://doi.org/10.1021/acs.biochem.1c00511
*Biochemistry* 2021, 60, 3027−3039

**Scheme 1. Reported Chemistry of RibA**

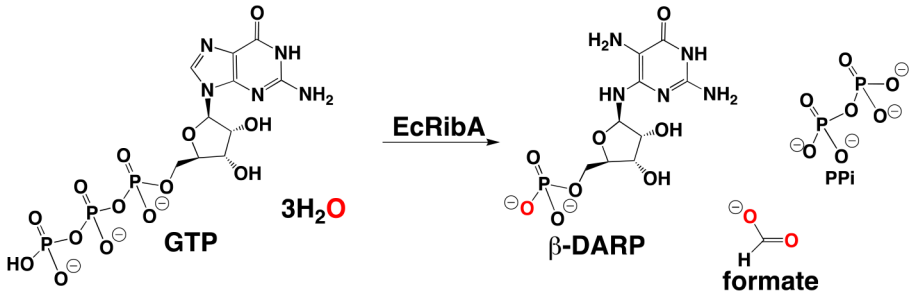


**Table 1. Expression and Purification Conditions**

| | EcRibA | EcPNP | ScPPase |
|---|---|---|---|
| Temperature equilibration time (hours) | 1 | 0 | 1 |
| Induction temperature (°C) | 20 | 37 | 16 |
| Induction time (hours) | 20 | 3.5 | 16 |
| Buffer A (resuspension) | 50 mM Tris, 2 mM βME pH 8.0 | 50 mM HEPES, 2 mM βME pH 7.5 | 50 mM HEPES pH 7.5 |
| Buffer B (wash) | 50 mM Tris, 50 mM NaCl, 2 mM βME, 10 mM Imidazole pH 8.0 | 50 mM HEPES, 50 mM NaCl, 2 mM βME, 10 mM Imidazole pH 7.5 | 50 mM HEPES pH 7.5 |
| Buffer C (elution) | 50 mM Tris, 50 mM NaCl, 2 mM βME, 300 mM Imidazole pH 8.0 | 50 mM HEPES, 50 mM NaCl, 2 mM βME, 300 mM Imidazole pH 7.5 | 50 mM HEPES, 300 mM Imidazole pH 7.5 |
| Buffer D (storage) | 25 mM Tris, 50 mM NaCl, 2 mM βME, 100 μM EDTA pH 8.0 | 25 mM HEPES, 100 mM NaCl, pH 7.5 | 50 mM HEPES pH 7.5 |

In this study we expanded the observations of Schramek et al. with *Escherichia coli* RibA (EcRibA) to identify the source of reported absorption changes that occur prior to hydrolytic steps when RibA is combined with GTP. Using PPi as a nonchromophoric activator, we show that these changes arise from perturbations of the underlying protein spectrum added to changes in the guanine absorption signal. We propose that the absorption shifts observed in the protein spectrum report a conformational activation prior to the catalytic hydrolysis chemistry. We also demonstrate that PPi is a slow substrate for RibA that is cleaved to form two Pi ions. Contrary to prior reports of the reaction stoichiometry,[1] when PPi is derived from turnover with GTP, it is hydrolyzed concomitant with the rate of formation of DARP. The slow substrate inosine triphosphate (ITP) was used to demonstrate that PPi is formed with nucleotide product(s) and that a slow hydrolytic chemistry at the hypoxanthine base allows for a complete PPi dissociation and ultimate hydrolysis by the independent and slow RibA pyrophosphatase (PPase) activity. We conclude that PPi is an intermediate, substrate, and activator for RibA that may serve to maintain the enzyme in the activated state but associates weakly with this form of the enzyme to prevent significant competition with GTP.

## MATERIALS AND METHODS

**Materials and Quantitation.** Lysogeny broth (LB) agar tablets were bought from Bio 101, Inc. Competent BL21-(DE3) cells were obtained from New England BioLabs. The Miller formulation of LB powder was obtained from Research Products International. Glycerol, β-mercaptoethanol (βME), isopropyl-β-D-1-thiogalactopyranoside (IPTG), guanosine, and pyrophosphate (PPi) were purchased from Acros Organics. Sodium chloride (NaCl), 2-(*N*-morpholino)ethanesulfonic acid (MES), ethylenediaminetetraacetic acid (EDTA), and tris(hydroxymethyl)aminomethane (Tris) were purchased from Fisher Scientific. Kanamycin and magnesium sulfate hydrate puratronic ($MgSO_4$) were purchased from Alfa Aesar. Guanosine triphosphate (GTP) and guanosine monophosphate (GMP) were purchased from MP Biomedical. 7-Methyl-6-thioguanosine (MESG) was purchased from Biosynth Carbosynth. Deuterium oxide ($D_2O$), inosine triphosphate (ITP), and inosine monophosphate (IMP) were purchased from TCI America. Talon superflow resin was from Cytvia. The ITP was found to be ∼40% contaminated with IDP and IMP and was purified using anion exchange chromatography. The mixture (10 mg) was dissolved in 5 mM Tris pH 8.5 and loaded onto a 2.5 cm × 12 cm Q-sepharose (Cytvia) column equilibrated in the same buffer. The nucleotides were separated using a gradient of 0−500 mM NaCl in the Tris buffer. The nucleotides eluted in sequence, and ITP was collected, lyophilized, and stored at −80 °C.

Concentrations of the purified proteins, substrates, and products were determined spectrophotometrically using the following extinction coefficients: GTP; $\varepsilon_{252}$ = 13 700 $M^{-1}$ $cm^{-1}$, GMP; $\varepsilon_{252}$ = 14 000 $M^{-1}$ $cm^{-1}$, ITP & IMP; $\varepsilon_{248}$ = 12 300 $M^{-1}$ $cm^{-1}$, DARP; $\varepsilon_{292}$ = 9500 $M^{-1}$ $cm^{-1}$,[6] MESG; $\varepsilon_{330}$ = 32 000 $M^{-1}$ $cm^{-1}$ at pH = 7.6,[12] EcRibA; $\varepsilon_{280}$ = 13 200 $M^{-1}$ $cm^{-1}$, *E. coli* purine nucleoside phosphorylase (EcPNP); $\varepsilon_{280}$ = 8940 $M^{-1}$ $cm^{-1}$, *S. cerevisiae* pyrophosphatase (ScPPase); $\varepsilon_{280}$ = 49 390 $M^{-1}$ $cm^{-1}$.[13]

**Expression and Purification of EcRibA, EcPNP, ScPPase.** Expression and purification of EcRibA, EcPNP, and ScPPase were achieved by small customizations of standard protocols. As such the methods are described generally, with specific details listed in Table 1. The genes for *E. coli* RibA and *E. coli* PNP were synthesized and subcloned into the pET28a+ expression plasmid by Genscript using Nde I and Xho I restriction sites to give the plasmids pEcRibA and pEcPNP, respectively. This placed both genes in frame with the sequence coding for a N-terminal 6His-tag linked by a thrombin cleavage site. The plasmid for *S. cerevisiae* PPase was a gift from the laboratory of Miguel Ballicora at


https://doi.org/10.1021/acs.biochem.1c00511
Biochemistry 2021, 60, 3027−3039

Loyola University Chicago. The gene for ScPPase was amplified by polymerase chain reaction (PCR) using oligonucleotides that included a sequence for a fused C-terminal 6His-tag and was subcloned into the pRSET-A plasmid using Nde I and Sac I restriction sites to give pScPPase. Each of these plasmids were transformed independently into competent BL21(DE3) *E. coli* cells. Cell stocks were prepared by transferring one cell colony to an LB growth culture with 25 $\mu$g/mL kanamycin (pEcRibA, pEcPNP) or 100 $\mu$g/mL ampicillin (pScPPase) and grown with shaking at 220 rpm at 37 °C until the culture showed signs of turbidity. Cell stocks of 1 mL were prepared by mixing 600 $\mu$L aliquots of the culture with 400 $\mu$L of 0.22 $\mu$m filtered 50% glycerol and stored in −80 °C.

To express EcRibA, EcPNP, and ScPPase, 100 $\mu$L of the BL21(DE3) cell stock was spread onto an LB agar plate with antibiotic selection as indicated above and incubated at 37 °C for 16 h. The resulting cell lawn was resuspended with sterile LB broth and used to inoculate 1 L of LB broth with the appropriate antibiotic as indicated above. Cells were grown at 37 °C with shaking (220 rpm) to an optical density at 600 nm of 0.6 and equilibrated to a specific temperature and induced as described in Table 1.

Protein purification was undertaken at 4 °C. Cells were harvested by centrifugation at 3500*g* for 35 min, and the cell pellet was resuspended in Buffer A. The cell slurry was lysed by sonication for 6 min using a Branson 450 sonifier set to 40 W. The cellular debris was separated by centrifugation at 10 000*g* for 1 h. The supernatant was loaded onto a Talon affinity column (10 × 1.25 cm) pre-equilibrated with Buffer B. Proteins were eluted using a 400 mL gradient of Buffer C and collected in 5 mL fractions. Fractions within the gradient elution that showed a significant absorption at 280 nm were pooled. Pure protein samples were concentrated and buffer-exchanged into Buffer D using Amicon Ultra-15, 10 kDa nominal molecular weight cutoff (NMWC) centrifugal filters. The concentrated sample was quantified by absorption and assayed prior to being stored at −80 °C.

**Transient-State Single-Turnover Observations of EcRibA with Nucleotide Triphosphates and PPi.** All transient-state observations of EcRibA were performed at 20 °C using a Hi-Tech stopped-flow spectrophotometer (TgK Scientific) that was configured for a 1:1 mixing ratio and a 1 cm path length. Throughout, all indicated concentrations are post mixing. Unless otherwise stated all reactions were performed in reaction buffer, 25 mM Tris, 50 mM NaCl, 5 mM $MgSO_4$, pH 8.0. The additives $\beta$ME (2 mM) or EDTA (100 or 150 $\mu$M) were included in specific experiments as indicated and were inconsequential to the observations. EDTA was used as a pretreatment to remove contaminant metals and was found to have no effect on the activity of EcRibA when Mg(II) was the only added metal ion (Figure S1). The Km for Mg was measured to be ∼20 $\mu$M (data not shown), and so concentrations of this metal ion equal to or above 1 mM were regarded as saturating. $\beta$ME was added in early preparations to maintain activity, though it was eliminated in latter preparations of EcRibA. The transient-state observation of the EcRibA reaction chemistry in the ultraviolet region is a composite due to overlapping absorption contributions from the nucleotide substrates and products and protein chromophores. To deconvolute these contributions we studied the behavior of EcRibA with GTP, ITP, and PPi.

The consumption of GTP by EcRibA was monitored at 252 or 250 nm using photomultiplier (PMT) detection. EcRibA (96 $\mu$M) in 25 mM Tris, 50 mM NaCl, 2 mM $MgSO_4$, 2 mM $\beta$ME, pH 8.0 was mixed with a range of concentrations of GTP (2.5−80 $\mu$M) in the same buffer. These data were fit to a linear combination of two exponentials according to the generalized expression eq 1. In this instance, $A_{Xnm}$ is the absorbance at any point in time at 252 or 250 nm, $\Delta A_n$ is the amplitude change associated with an observed rate constant $k_{obsn}$ defined for a specific phase and concentration of GTP. *C* is the absorbance at infinite time, and the term *x* in the summation refers to the number of phases fit.

$$A_{Xnm} = \left(\sum_{n=1}^{x} \Delta A_n\left(e^{-k_{obsn}t}\right)\right) + C \quad (1)$$

The reaction of EcRibA with GTP was also monitored using a charged couple device (CCD) that records all wavelengths between 240 and 850 nm. In initial attempts to observe only changes associated with the guanine chromophore, 40 $\mu$M EcRibA was used to baseline the instrumnet prior to the addition of GTP. EcRibA (40 $\mu$M) and GTP (48 $\mu$M) were mixed, and spectra were collected for 100 s. These data were analyzed using the singular value decomposition (SVD) routine available in KinTek Explorer software (KinTek Corp.)[14,15] to deconvolute the composite spectral data sets. The model of a linear two-step irreversible system was used and did not account for substrate binding that was assumed to be rapid. The time zero spectrum was subtracted from the intermediate spectrum to obtain a difference spectrum that reports the absorption changes associated with the first phase.

For most instances the reaction of GTP or ITP with EcRibA was observed by mixing 100 $\mu$M enzyme with 40 $\mu$M substrate in reaction buffer and monitoring at 250−252 and ∼290−310 nm for 100 s. This ratio of enzyme and substrate yields a net single turnover but is not based on a measured dissociation constant for the EcRibA·XTP complex and so does not report intrinsic rate constants. The wavelengths used, respectively, report changes in the purine/enzyme spectra and pyrimidine mononucleotide product. The data obtained were fit to linear combinations of exponentials (eq 1).

PPi is also a substrate for RibA and has no spectrophotometric absorption in the middle-UV range. Therefore, when titrating PPi to a constant concentration of enzyme, the absorption changes observed report only changes to the enzyme spectrum. EcRibA (100 $\mu$M) with 150 $\mu$M EDTA was mixed with a range of concentrations of PPi (0−499 $\mu$M) and monitored at 252 nm for 600 s. These conditions provide neither ideal single-turnover or pseudo-first-order conditions and were not fit with the purpose of determining intrinsic rate constants. Instead, the resulting traces were fit to a single exponential (eq 1) to obtain estimates of the amplitudes associated with the first phase observed. The resulting $\Delta A$ values were plotted against the PPi concentration. These data were fit to eq 2 to provide an estimate of the PPi dissociation constant. In eq 2, [PPi] is the concentration of PPi, [EcRibA] is the concentration of EcRibA, and $K_{PPi}$ is the dissociation constant for the EcRibA·PPi complex. The data were also fit to the Hill equation (eq 3) to discern evidence of a cooperative subunit activation.


https://doi.org/10.1021/acs.biochem.1c00511
*Biochemistry* 2021, 60, 3027−3039

$$[\text{EcRibA·PPi}] = 0.5 \times \{([\text{PPi}] + [\text{EcRibA}] + K_{\text{PPi}}) - \sqrt{([\text{PPi}] + [\text{EcRibA}] + K_{\text{PPi}})^2 - (4[\text{PPi}] + [\text{EcRibA}])}\} \quad (2)$$

$$\Delta A_{\text{xnm}} = \frac{\Delta A_{\text{max}}[\text{PPi}]^n}{K_{1/2}{}^n + [\text{PPi}]^n} \quad (3)$$

Using CCD detection, the spectrophotometric changes that occur as the enzyme interacts with PPi were monitored. However, we observed a light-induced artifact centered around 300 nm when the sample was excited simultaneously with all wavelengths between 240 and 850 nm. This artifact undermined our capacity to isolate the spectra of each individual species. For this reason, scanning photomultiplier detection was used to capture individual spectra at specific times. For each spectrum, 100 $\mu$M EcRibA with 150 $\mu$M EDTA was mixed with 100 $\mu$M PPi and observed at 252 nm. Initially, a spectrum of the RibA and PPi mixture was collected in reaction buffer without added $MgSO_4$ (preventing catalysis) to obtain a representation of the zero-time spectrum. To capture the midpoint spectrum, EcRibA and PPi were combined in reaction buffer, and a spectrum was acquired after 10 s. To capture the end-point spectrum the reaction was monitored for 4000 s, at which time a spectrum was taken. The magnesium-free spectrum was then subtracted from the midpoint reaction spectrum to obtain a difference spectrum that reports the changes associated with the first phase.

PPase was used to demonstrate the effect of exogenous PPi hydrolysis on the observed kinetics of EcRibA reacting with GTP and PPi. ScPPase has a turnover number that is ~2600-fold more rapid than EcRibA, and even at low concentrations it will rapidly hydrolyze PPi that dissociates from EcRibA.[16] Using the stopped-flow spectrophotometer, 100 $\mu$M EcRibA with 150 $\mu$M EDTA in reaction buffer was mixed with 40 $\mu$M GTP with and without 2 $\mu$M PPase. The reaction was monitored at 252 nm to observe the activation and consumption of GTP and at 292 nm to observe the production of DARP. The data obtained with and without added PPase were fit analytically to linear combinations of exponentials to provide a comparison of observed rates and amplitudes (eq 1).

The spectrophotometric changes associated with EcRibA's interaction with PPi were also observed with and without ScPPase using double-mixing stopped-flow methods. While monitoring at 252 nm, 100 $\mu$M EcRibA with 150 $\mu$M EDTA was mixed with 25 $\mu$M PPi and allowed to age for 0.1 s, then mixed with reaction buffer and monitored for 2000 s. This was used as a reference reaction prior to the addition of PPase. The reaction was repeated but mixed with a concentration of ScPPase that was defined empirically by a titration to be sufficiently low that the PPase activity of both enzymes was similar. With a 0.1 s age time this reaction was monitored for 2000 s. To measure the rate of EcRibA relaxation in the absence of PPi, 100 EcRibA was mixed with PPi as described above and aged for 25 s before being combined with 1 $\mu$M ScPPase. The data obtained were fit to a single exponential to determine the rate constant for an enzyme conformational relaxation that occurs in the absence of PPi.

**Evidence of Binding Competition of PPi for the GTP Binding Site.** To demonstrate that PPi and GTP bind in the same cavity within the EcRibA active site, steady-state analyses were undertaken with GTP as a substrate at various concentrations of PPi. Using the stopped-flow spectrophotometer, 1 $\mu$M EcRibA was combined with a range of GTP concentrations (10−640 $\mu$M), and the rate of turnover was measured at 292 nm based on the accumulation of DARP. The observed rate was evaluated during the steady state between 100 and 400 s. The rates obtained were plotted versus the GTP concentration and fit to eq 4 in which $v$ is the observed rate of reaction in units of concentration per unit time, [EcRibA] is the concentration of enzyme, [GTP] is the concentration of GTP, $k_{\text{cat}}$ is the turnover number for EcRibA, and $K_{\text{m}}$ is the Michealis constant.

$$\frac{v}{[\text{EcRibA}]} = \frac{k_{\text{cat}}[\text{GTP}]}{K_{\text{m}} + [\text{GTP}]} \quad (4)$$

This analysis was repeated in the presence of a range of PPi concentrations (20−640 $\mu$M). The nested set of curves was fit globally to a competitive binding model using the inbuilt routine within Prism software (Graphpad) to obtain the Km for PPi.

**Acid Quench and HPLC Product Analysis of the EcRibA Reaction with ITP.** The slow rate of turnover observed with ITP facilitated an acid quench and subsequent product analysis to evaluate the time-dependent accumulation of specific species during a single turnover. In this experiment 2825 $\mu$L of reaction buffer was combined with 128 $\mu$L of EcRibA (100 $\mu$M final) and mixed. To this solution 247 $\mu$L of ITP (40 $\mu$M final) was added and mixed. At specific times (10−14 000 s) 200 $\mu$L of the reaction was withdrawn and combined with 20 $\mu$L of 2 M trichloroacetic acid (TCA) and vortexed. The quenched samples were centrifuged at 12 000 rpm for 5 min, and 100 $\mu$L of the supernatant was withdrawn and neutralized by the addition of 6.2 $\mu$L of 3 M NaOH and vortexed. A control containing ITP in the reaction buffer was quenched in an equivalent manner to evaluate the extent of hydrolysis of ITP in the presence of TCA. The neutralized samples were analyzed using reverse-phase high-performance liquid chromatography (HPLC). For each, 10 $\mu$L of the sample was injected onto a Waters Xterra C18 column (4.6 × 250 mm, 5 $\mu$m particle size) coupled to a Shimadzu Prominence HPLC system and separated using a mobile phase of 0.3% (v/v) phosphoric acid, 1% triethylamine, 0.8% isopropyl alcohol pH 7.0. Chromatograms of the reaction mixture were acquired at 248 and 300 nm. The ITP and IMP components were identified and quantified from standard curves for both molecules. The 5-amino-6-$\beta$-pyrimidinone 5′-phosphate (ARP) product was quantified only by the peak area, and the concentration was determined by the difference. This procedure does not account for an epimerization of this product that both broadens the peak observed and is expected to minimally alter the absorption spectrum.

Chromatograms were normalized to the area of the peak observed for the buffer. The resulting peak areas obtained were used to deduce reaction component concentrations computed for each time point based on the ITP and IMP standard curves. The data were plotted versus time, and the decay of ITP and the accumulation of both IMP and the ARP product were fit to a single exponential according to eq 1.

**Indirect and Direct Demonstrations of EcRibA Pyrophosphatase Activity.** A demonstration of the production of Pi as a product of the EcRibA reaction was accomplished using MESG with purine nucleoside phosphorylase (EcPNP) and by a direct observation of the $^{31}$P resonances of PPi and Pi in the presence of EcRibA.


https://doi.org/10.1021/acs.biochem.1c00511
Biochemistry 2021, 60, 3027−3039

Excess EcPNP activity was used to consume free inorganic phosphate originating from the from RibA hydrolysis reaction(s). With either GTP or PPi as the substrate, the PPase activity of EcRibA was observed using a coupled assay in which the MESG nucleoside served as the purine substrate for EcPNP, thereby generating the chromophore 2-amino-6-mercapto-7-methylpurine, which absorbs at 360 nm, and ribose 1-phosphate.[12] To establish a standardized response for this assay under the conditions used, the change in absorbance at 360 nm was measured for a range of Pi concentrations in the presence of 5 $\mu$M EcPNP and 200 $\mu$M MESG in reaction buffer. The amplitudes observed were plotted against the Pi concentration, and the data were fit to a straight line from which the extinction coefficient change was obtained from the slope. The EcPNP was titrated to identify at what concentration it would not be a limiting factor in the coupled assay.

Initially a sample of 100 $\mu$M EcRibA was mixed with 40 $\mu$M GTP in 50 mM Tris, 50 mM NaCl, and 5 mM $MgSO_4$ pH 8.0 and monitored at 252 nm for ∼100 s as a control. The inorganic phosphate assay was performed in a similar manner with the addition of EcPNP and MESG. MESG was prepared immediately prior in 10 mM MES pH 6.0 and filtered (0.22 $\mu$m). As such the assay conditions were dominated by the buffer used with EcRibA. The inorganic phosphate reaction included 100 $\mu$M EcRibA, 150 $\mu$M EDTA, and 66 $\mu$M EcPNP mixed with 40 $\mu$M GTP and 400 $\mu$M MESG. The production of the MESG-free base by EcPNP dependent on EcRibA turnover was monitored at 360 nm for ∼100 s. The data were collected and compared to the original 252 nm trace to determine which of the observed phases corresponded to phosphate release. An identical reaction was performed with the addition of 5 $\mu$M ScPPase. Prior to each coupled assay, the stopped-flow system was scrubbed with ScPPase, EcPNP, and guanosine to remove residual PPi and Pi that had adhered to the internal surfaces of the instrument. An additional control reaction in which 66 $\mu$M PNP was mixed with 400 $\mu$M MESG and buffer and monitored at 360 nm was also undertaken to assess a signal from the background phosphate.

A subsequent reaction was performed using PPi rather than GTP as the substrate for EcRibA. A sample of 100 $\mu$M EcRibA was mixed with 25 $\mu$M PPi in reaction buffer. The consumption of PPi by EcRibA turnover was monitored at 252 nm for ∼2000 s. The phosphate assay was performed by mixing 100 $\mu$M EcRibA, 150 $\mu$M EDTA, and 75 $\mu$M PNP with a sample containing 25 $\mu$M PPi and 200 $\mu$M MESG. The production of the MESG-free base by PNP during the EcRibA turnover was monitored at 360 nm for ∼2000 s. The data collected were compared to the original 252 nm trace to determine in which phase Pi was released.

**$^{31}$P NMR Observation of EcRibA Turnover with GTP, ITP, and PPi.** Both PPi and ITP induce slow catalytic processes by EcRibA. $^{31}$P NMR was used to observe the conversion of PPi to Pi as a formal proof of this activity and to observe the accumulation and decay of species in a net single-turnover reaction with ITP. The end-point consumption of GTP was also undertaken to confirm that the product, Pi, accumulates at a rate that is catalytically relevant and more rapid than when PPi is the sole substrate. Each observation was performed using a Bruker A600 NMR instrument fitted with a cryoprobe. Each spectrum recorded included 128 FIDs (FID = free induction decay) and was acquired over a period of 7 min and 50 s at 25 °C. When successive spectra were recorded to observe the catalytic process with time, each acquisition was separated by a 1 s delay. Reactions were performed in 25 mM Tris, 50 mM NaCl, 5 mM $MgSO_4$, 10% $D_2O$ pH 8.0. The dominant volume (enzyme or substrate) of each reaction was added to a 188 mm NMR tube and locked, tuned, and shimmed prior to the addition of the initiating reactant (enzyme or substrate) using a 215 mm stainless steel 20-gauge luer needle attached to a 1 mL plastic syringe. The initiating solution was mixed with the solution in the NMR tube by drawing the entire sample into the syringe four times before the reaction was returned to the instrument and data collection was initiated. This process consumed ∼3 min 30 s of the reaction time.

To monitor the conversion of PPi to Pi by EcRibA a sample of 550 $\mu$L of 1.27 mM PPi was added to the NMR tube and initiated with the addition of 150 $\mu$L of 466 $\mu$M EcRibA (1 mM PPi, 100 $\mu$M EcRibA final). This reaction was monitored by collecting 46 spectra over 360 min. For the conversion of ITP to ARP, IMP, and Pi, a sample of 3 mM EcRibA in 550 $\mu$L was added to the NMR and shimmed and then mixed with 150 $\mu$L of 8.38 mM ITP (2.36 mM EcRibA, 1.79 mM ITP final). This reaction was monitored by collecting 70 spectra over 550 min. The conversion of GTP to DARP and Pi was too rapid to be observed in real time by NMR. For this reason, the end point of the reaction was observed 11 min after the initiation. A sample of 550 $\mu$L of 1.9 mM EcRibA was combined 150 $\mu$L of 4.6 mM GTP (1.5 mM EcRibA, 0.985 mM GTP final), and a single spectrum was acquired.

## RESULTS AND DISCUSSION

The study of EcRibA is complicated by inherent limitations to the application of conventional absorption-based transient-state kinetic approaches to describe the chemistry. These limitations include a complex multistep reaction that is largely shrouded by slow initial steps and modest extinction coefficient changes from intensely absorbing and overlapping enzyme and substrate chromophores. As such events prior to the production of DARP cannot be studied by systematic titration of either substrate or enzyme to saturation without the transmitted light diminishing to a level that exceeds the detection limits of the instruments used for observation. These limitations negate the measurement of dissociation constants by titration and limit the ability to observe single-turnover reactions in which the substrate is saturated in the enzyme based on a known $K_d$ value. For these reasons we chose to study the chemistry of EcRibA within the available observational limits by monitoring the enzyme activation and turnover under subsaturating, net single-turnover conditions, where the enzyme is in excess but only a fraction of the substrate is bound when the two are initially combined.

**Transient-State Kinetics of EcRibA with GTP.** In prior investigations of EcRibA, Schramek and co-workers characterized multiple aspects of the GTP cyclohydrolase II reaction.[2,5,6] One of these studies included a transient-state spectrophotometric investigation and a spectral deconvolution. In this analysis it was revealed that two phases are observed in single-turnover reactions of EcRibA and that the spectra obtained suggested that the first phase observed was a blue-shift in the GTP guanine chromophore induced by binding to the RibA active site. Rapid quench and product analysis was used to show that GTP consumption occurred in the second phase and was concomitant with DARP formation. However, the conclusions also indicated that it was equally likely that the


https://doi.org/10.1021/acs.biochem.1c00511
Biochemistry 2021, 60, 3027−3039

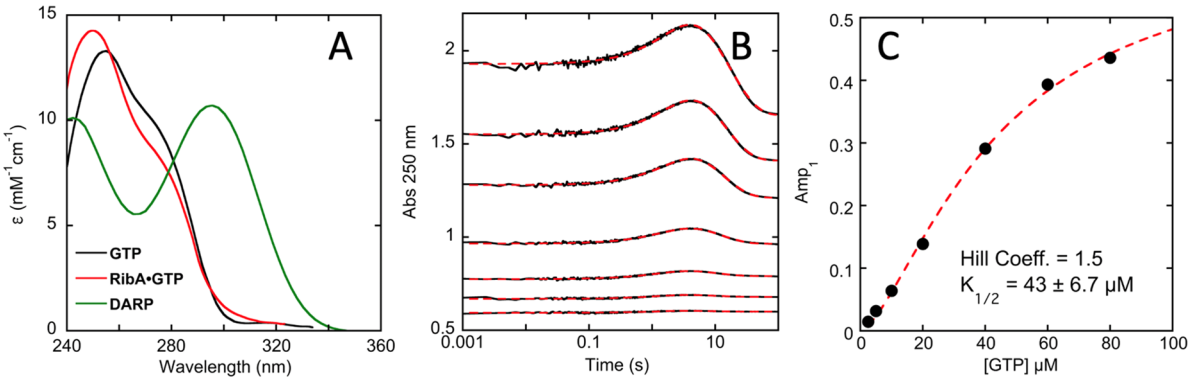


**Figure 1.** Transient-state kinetics of WT RibA with GTP. (A) Spectra extracted from ref 6. (B) RibA (96 $\mu$M final) was mixed with GTP (2.5, 5,10, 20, 40, 60, and 80 $\mu$M final) and observed at 250 nm. These data were fit (red dashed line) to eq 1, which describes a linear combination of two exponentials. The amplitudes for the first phase were plotted against the GTP concentration in (C) and fit to the Hill binding equation, eq 3.

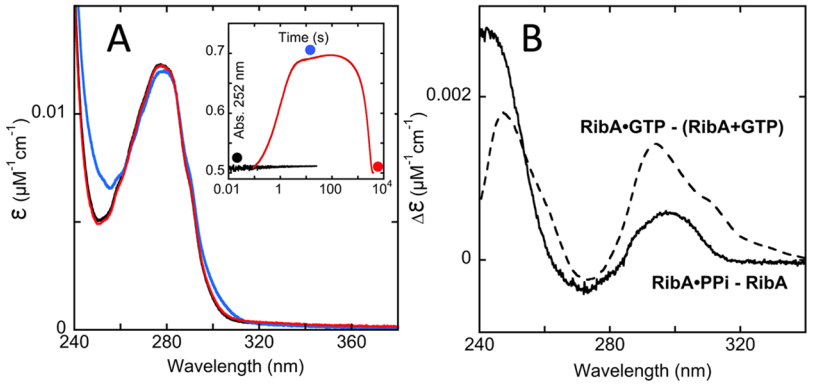


**Figure 2.** Transient-state difference spectra of WT RibA with PPi and GTP. RibA (100 $\mu$M) was mixed with PPi (100 $\mu$M) and 5 mM Mg(II). (A) Spectra of RibA obtained at 0 (black), 10 (blue), and 4000 (red) seconds (as indicated) for the reaction depicted in the inset. (inset) The reaction observed at 252 nm (red trace). The reaction was also observed in the absence of added Mg(II) (black trace) to obtain the spectrum of the nonactivated enzyme. (B) Difference spectra for $t$ = 10 s spectrum minus $t$ = 0 s spectrum overlaid with the difference spectrum for RibA·GTP minus GTP from spectra depicted in Figure 1A.

shift observed in the first phase was a result of changes in the protein spectrum that overlap with the GTP absorption.[6] We revisited the conclusions made in these prior studies and expanded the characterization of the reaction by both titrating GTP and identifying the source of the absorption changes that occur in the first phase observed in a single turnover. In Figure 1A the deconvoluted spectra of Schramek et al. are presented for reference.

Figure 1B depicts the traces observed at 250 nm when GTP is titrated to EcRibA. These data were described well when fit to two exponentials and qualitatively show that the first phase is slow relative to rates normally associated with ligand binding. The observed rate constant of the first phase does not titrate significantly with GTP concentration; however, in the presence of excess EcRibA this cannot be taken as evidence that this step necessarily occurs after binding. As indicated by Schramek the subsequent phase results in the accumulation of the product, DARP, that is observed at this wavelength as a loss of the guanine absorption signal. When these data were fit analytically to two exponentials a plot of the dependence of the first phase amplitude change was best fit to the Hill equation as a result of a small amount of a sigmoidal character (Figure 1C). The fit returns a Hill coefficient of 1.5 indicating a modest cooperativity for the two protomers of the EcRibA dimer with the binding of GTP. Previous evidence of cooperativity in the reaction of EcRibA was reported by Bacher and co-workers, who observed a Hill coefficient of 1.3 in steady-state observations.[5] The structural origin of this apparent intersubunit cooperativity is not known, as all available X-ray crystal structures have the same peptide conformation for all residues resolved.[3,17] These structures were solved either in the absence of Mg or with a nonsubstrate GTP analogue ligand and, therefore, may reflect a nonactivated state of RibA. The $K_{1/2}$ value determined from the fit was 43 $\mu$M, similar to the $K_m$ of 32 $\mu$M measured in steady state for GTP that should closely approximate the $K_{GTP}$ value given that the turnover number is slow at ~0.06 $s^{-1}$ (Figure 1B).[6] Moreover, if we assert that the activated enzyme predominates in the steady state, as a result of a relatively slow conformational relaxation (see below), GTP is binding to a different form of the enzyme in such experiments, and yet the apparent binding constants are similar.

**EcRibA Pyrophosphatase Activity.** Initial evidence of an induced fit prior to the catalysis was obtained by adding the proposed product PPi to RibA and observing the protein spectrum (Figure 2A). The data obtained indicated that RibA binds PPi and displays a similar induced-fit process to that observed with GTP. However, the trace revealed that the enzyme returned to its initial spectrum indicating that equilibrium binding and irreversible catalysis were occurring (Figure 2A inset). A comparison of the difference spectra obtained for the first phase in the presence of PPi or GTP


https://doi.org/10.1021/acs.biochem.1c00511
Biochemistry 2021, 60, 3027−3039

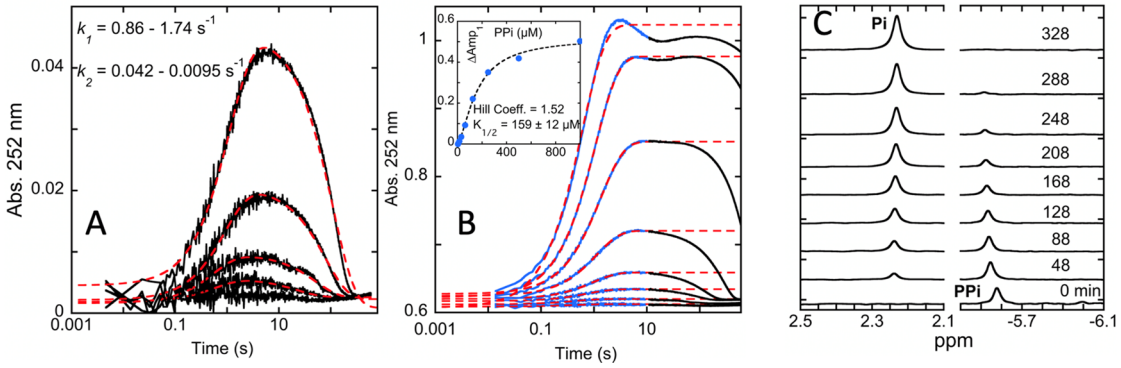


**Figure 3.** PPi as a substrate for RibA. (A) RibA (100 $\mu$M final) was mixed with PPi (3.9, 7.8, 15.6, 31.2, and 62.4 $\mu$M final) and observed at 252 nm. The data were fit to a linear combination of two exponentials (eq 1). (B) RibA (100 $\mu$M final) was mixed with PPi (3.9, 7.8, 15.6, 31.2, 62.4, 124.8, 249.6, and 499 $\mu$M final) and observed at 252 nm. For both (A) & (B), the original traces showed a degree of positional variability and were artificially offset in the figure to commence at approximately the same absorbance value. For (B) the first phase observed (indicated in blue) was fit to a single exponential expression (eq 1) to obtain the amplitudes as a measure of equilibrium binding for PPi. (inset) Ligand-binding isotherm based on the amplitudes for the first phase observed in (B) fit to the Hill binding equation (eq 3). (C) $^{31}$P in vivo multifunctional magnetic resonance spectroscopy evidence of EcRibA pyrophosphatase activity. EcRibA (100 $\mu$M final) was combined with PPi (1000 $\mu$M final) in reaction buffer with 10% $D_2O$ and observed by collecting 128 FIDs per spectrum over the time indicated.

indicated that the changes were qualitatively similar (Figure 2B). It is not expected that the difference spectra would be the same, as, unlike GTP, PPi offers no chromophore at these wavelengths. The GTP difference spectrum is therefore assumed to be additive for changes in both the enzyme and guanine absorption spectra.

To further investigate the apparent catalytic behavior of RibA in the presence of PPi, this ligand was titrated to RibA, and the reaction was observed at 252 nm (Figure 3). In this experiment the range of PPi concentrations used was pseudo-first-order in enzyme and net single turnover at low PPi concentrations, while the high PPi concentrations induced multiple turnovers. Though the rate of the first phase observed increases with PPi the data cannot be analyzed as though they were a systematic pseudo-first-order set. As such only the low concentration, net single-turnover data obtained for 7.8−62.4 $\mu$M PPi were fit using a linear combination of two exponentials (Figure 3A). These data indicate that the overall catalytic process with PPi can be fit to two phases but that none provide the measurement of intrinsic rate constants. Nonetheless, the data indicate a conformational perturbation process of ∼1−2 s$^{-1}$ in response to PPi binding and a slowing conformational return of 0.04−0.01 s$^{-1}$ after or coincident with catalysis. As PPi was titrated to higher concentrations the amplitude of the first phase increased to a limit and revealed added complexity (Figure 3B).

The amplitudes were estimated by single exponential fits to the first phase only. These values were plotted against the PPi concentration and fit to the Hill equation (eq 3) to obtain a Hill coefficient equal to that observed with GTP and a $K_{1/2}$ of 160 $\mu$M (Figure 3B inset). Given that the catalysis is slow, this value was used as an approximation of the binding constant for the EcRibA·PPi complex. Weak binding for PPi accounts for the lack of consistency in the rate constants determined from the enzyme-monitored single-turnover data of Figure 3A. The apparent slowing of the second phase with an increased PPi concentration was concluded to be a result of prolonged activation that arises from the dissociation of PPi from a conformationally activated state (see below). Though $K_{1/2}$ values do not represent $K_d$, the apparent weak binding predicts that the data represented in this figure are from a low fractional EcRibA·PPi complex at equilibrium such that lagging binding processes to form the complex contribute to the kinetic observation. The association of EcRibA with PPi was also evaluated using pseudo-first-order ratios of PPi (Figure S2). These data indicate a linear dependence of the first observed rate constant on the PPi concentration with a positive $y$-intercept that yields an apparent $K_d$ for PPi of 50 $\mu$M. In addition, the amplitude of the first phase decreases with increasing PPi concentration signifying an inhibitory binding mode for PPi. The linear dependence indicates either that we are observing binding in the first phase or that a rapid conformational change is induced by PPi binding. The latter of these possibilities was regarded as more probable, as the overall extinction coefficient changes in the protein spectrum are large (∼2000 M$^{-1}$ cm$^{-1}$), suggesting pronounced conformational alterations.

To verify that EcRibA exhibited a slow pyrophosphatase activity, $^{31}$P NMR was used to track the consumption of 1 mM PPi by 100 $\mu$M RibA. These data show that all added PPi was converted to inorganic phosphate, establishing a hitherto unreported activity for this enzyme (Figure 3C). The rate of turnover was obtained by plotting the peak area for Pi standardized to the area for a complete conversion at 328 min against time and fitting the linear portion (24−128 min). The slope of this line indicated a turnover number for PPi of (124 ± 1.2) × 10$^{-6}$ s$^{-1}$, 6 orders of magnitude faster than the rate of PPi hydrolysis in the presence of Mg alone[18] but considerably slower than the value determined for relaxation from the net single turnover (Figures 3A & 4B). The apparent slow turnover number measured from the NMR data suggests that high concentrations of PPi are inhibitory for the EcRibA PPase activity (Figure S2). One potential explanation is that PPi as a substrate can bind in either the $\alpha-\beta$ or $\beta-\gamma$ phospho group binding sites relative to the GTP association but is cleaved more slowly or not at all in one of these two binding modes, and this site is populated only at higher PPi concentrations. To demonstrate that PPi and GTP compete for the same binding site, the influence of increasing PPi concentration on GTP steady-state kinetics was evaluated (Figure S3). These data were well-described by a competitive substrate model and fit to determine a $K_m$ for PPi of 23 $\mu$M.[19] This agrees well with the


https://doi.org/10.1021/acs.biochem.1c00511
Biochemistry 2021, 60, 3027−3039

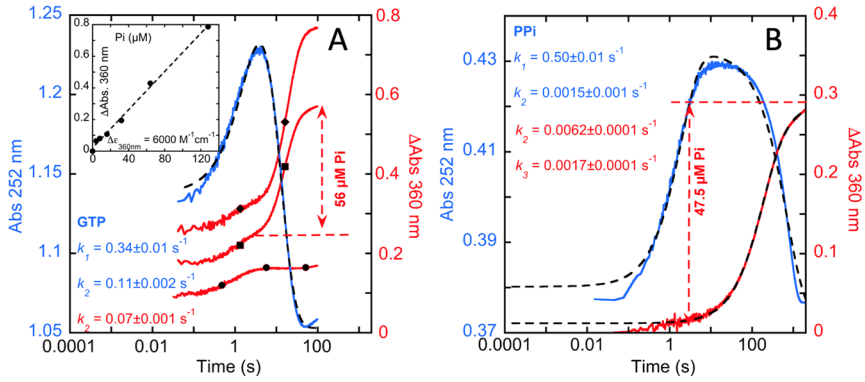


**Figure 4.** Transient-state kinetics of phosphate detection for RibA reacting with GTP and PPi. (A) RibA (100 $\mu$M) was mixed with GTP (40 $\mu$M final). The traces depict data at 252 nm (blue line) that report the net single-turnover reaction of EcRibA and detection of phosphate evolved from this reaction at 360 nm (red lines) using purine nucleoside phosphorylase (66 $\mu$M) and MESG (400 $\mu$M). The MESG traces shown are for background phosphate (●), in the presence of GTP only (■), and for GTP and ScPPase (10 $\mu$M) (◆). (inset) Standardization of the response of the coupled assay. (B) RibA (100 $\mu$M) was mixed with PPi (25 $\mu$M). The traces depict data at 252 nm (blue line) for an apparent net single turnover by RibA pyrophosphatase activity and the detection of phosphate evolved from this reaction at 360 nm (red line) using purine nucleoside phosphorylase (75 $\mu$M) and MESG (200 $\mu$M).

measured dissociation constant for PPi binding to the resting enzyme, demonstrating that PPi has a similar affinity for EcRibA in the proposed conformationally activated form that is assumed to predominate in the steady state (Figures S2 & S3). Collectively the data presented in Figures 1−3 suggest that EcRibA undergoes a conformational activation in the presence of the $\beta$ and $\gamma$ phospho groups of GTP. This activation is not observed with GDP or GMP (data not shown) but is apparent with PPi, where the activation induces the catalytic hydrolysis of the phosphodiester bond, implying that such an activity is potentially part of a catalysis with the native substrate, GTP (see below).

**Real-Time Detection of Pi as a Product.** To establish both the native production of Pi and correlate its accumulation with a specific phase observed in a single turnover, the reactions of GTP and PPi with EcRibA were observed in the transient state with and without EcPNP and MESG nucleoside. The EcPNP, MESG reaction reports the production of Pi as the MESG base is liberated from the nucleoside.[12] Figure 4A depicts the reaction of EcRibA with GTP observed at 252 nm. The GTP turnover reaction could be described adequately by a fit to two exponentials with rate constants of 0.34 and 0.11 $s^{-1}$ that are assigned to an induced-fit conformational activation and catalysis to form DARP, respectively.

These rate constants are likely to approximate intrinsic values, as the GTP is expected to be close to uniformly bound by the EcRibA upon mixing. Supposing the $K_{1/2}$ value of 43 $\mu$M for GTP is an approximation of $K_{GTP}$, the 40 $\mu$M GTP in this reaction would be 65% bound to the 100 $\mu$M EcRibA post mixing. When the same reaction was observed at 360 nm in the presence of MESG and EcPNP, the rate of MESG base elimination at 0.07 $s^{-1}$ was similar to that observed for the production of DARP. In addition, the amplitude of the MESG reaction corresponded to 56 $\mu$M Pi, largely inconsistent with the 40 $\mu$M GTP consumed in the reaction; this discrepancy will be addressed below. These data indicate that the rate of Pi production by EcRibA is correlated with the limiting rate of catalysis and as such Pi accumulates with a catalytically relevant rate.

The liberation of Pi from a net single-turnover reaction of EcRibA with the PPi substrate was also evaluated using the EcPNP, MESG reporter assay. The PPi single-turnover reaction was fit to a two-exponential expression and returned rate constants of 0.50 and 0.0015 $s^{-1}$ (Figure 4B). The $K_d$ value for the EcRibA·PPi complex predicts that 62% of the added PPi is bound by EcRibA post mixing (Figure S2). The rate of the dominant phase for MESG base elimination was 0.0017 $s^{-1}$ and correlates well with the rate of the final phase observed at 252 nm. The amplitude of this phase indicates 48 $\mu$M Pi production (95%), consistent with the 25 $\mu$M PPi used in this experiment.

These data reveal that the hydrolysis of PPi is a native chemistry of EcRibA and occurs with GTP as a substrate at a catalytically relevant rate. In the absence of GTP, PPi is a substrate for EcRibA that conformationally activates the enzyme with a similar rate to that observed with GTP but then cleaves the phosphodiester bond approximately 50-fold more slowly in the absence of the associated chemistry at the GMP purine. Interestingly, PPi cannot induce RibA to convert GMP to DARP. When PPi (25 $\mu$M) and GMP (300−700 $\mu$M) are added simultaneously to the enzyme (100 $\mu$M), a binding/conformational activation is observed, but no increase at 292 nm for the formation of DARP occurs (data not shown). This suggests that, in the conformationally activated state, the enzyme has a low affinity for GMP and in the aggregate that the $\beta$ and $\gamma$ phospho groups have the greatest contribution to the binding energy and hence substrate recognition. However, this is not absolute as neither adenosine triphosphate (ATP) nor triphosphate induce a conformational activation (data not shown).

**Evidence of Dissociable PPi in Turnover with GTP and PPi.** In Figure 5A we see that, when the reaction is monitored past 100 s, an additional slow phase is observed after the DARP formation is complete. This phase is enhanced in amplitude, prolonged with the addition of PPi, and eliminated with the addition of ScPPase.

This reveals not only that PPi that formed in the native GTP reaction is largely converted to Pi during turnover but also that some fraction dissociates from the activated enzyme such that it can be consumed either by EcRibA or exogenous PPase activity. This indicates that there exist two fates for PPi formed in the EcRibA reaction. The majority is converted to Pi during the production of DARP, and the remainder dissociates and is rebound and hydrolyzed after the DARP production and


https://doi.org/10.1021/acs.biochem.1c00511
Biochemistry 2021, 60, 3027−3039

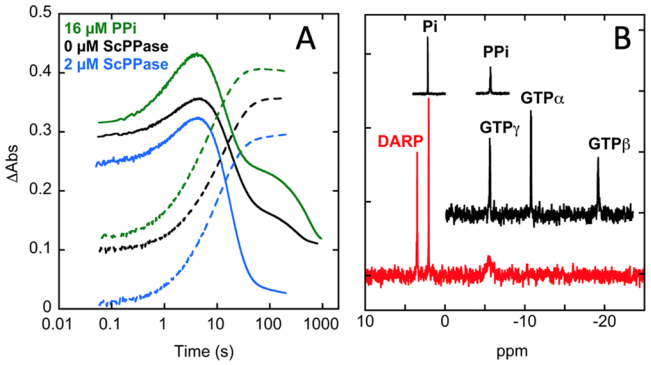


**Figure 5.** Evidence for native pyrophosphatase activity. (A) RibA (100 $\mu$M final) was mixed with GTP (40 $\mu$M final) and observed at 252 nm (solid lines) and 292 nm (dashed lines). The traces shown depict the effect of pyrophosphate on the observed kinetics. As indicated the green traces were acquired with exogenous PPi (16 $\mu$M final), the black traces were recorded without additives, and the blue traces were recorded with ScPPase (2 $\mu$M final). (B) Net single turnover of GTP monitored by $^{31}$P NMR. RibA (1500 $\mu$M final) in reaction buffer with 10% $D_2O$ was mixed with GTP (985 $\mu$M final) in the same buffer. The 128 FID $^{31}$P NMR spectrum was then recorded within 660 s of mixing by using a Bruker A600 NMR instrument. Standards for GTP (1 mM) and PPi and Pi (both 2 mM) were collected in the same manner.

dissociation. To confirm this, the GTP reaction was monitored as an end point using $^{31}$P NMR (Figure 5B). The single spectrum obtained 660 s after the reaction was initiated definitively shows that only DARP and Pi are detectable products in the reaction. This observational time is too short for PPi to have been consumed as a separate substrate and is consistent with it being hydrolyzed as an intermediate (Figure 3C), as the MESG data had indicated (Figure 4A). We propose that the small amount of PPi observed in the GTP reaction is from an uncoupling that forms a minor fraction of GMP as previously reported.[5,8]

To establish whether PPi dissociates from EcRibA during the independent PPase reaction, the signal associated with binding/conformational activation and relaxation was observed in the presence and absence of the ScPPase. In Figure 6A the effect of mixing EcRibA with PPi and a low ScPPase concentration is depicted.

These data indicate that, when the net ScPPase activity is comparable to that of the EcRibA PPase activity, ScPPase curtails the activation reaction and returns the enzyme to the resting state more rapidly (in this instance ~50-fold). This was interpreted as PPi binding and activating EcRibA but being free to dissociate and become hydrolyzed by ScPPase such that the equilibrium concentration of the activated EcRibA·PPi could not be sustained prior to the slow EcRibA PPase activity. This signal was also used to observe the intrinsic rate of relaxation by first mixing EcRibA with PPi, aging it for 25 s to maximally activate the enzyme, and then mixing it with excess ScPPase activity (Figure 6B). The absorption data obtained indicate a relaxation rate of 0.54 $s^{-1}$, ~300-fold faster than the predicted turnover number of EcRibA with PPi (Figure 3A). These data contrast with the EcRibA GTP reaction, where no evidence of an accelerated relaxation was induced by the addition of excess ScPPase activity (Figure 5A). Given that Pi is observed to form in the second phase of turnover with GTP (Figure 4A), it can be concluded that PPi formed in the native reaction is not as free to dissociate and that the relative rapid conformational relaxation observed is contingent on both DARP formation and PPi hydrolysis.

**Transient State Kinetics and Product Analysis of EcRibA with ITP.** Inosine triphosphate differs from GTP in that the purine base does not have an amino substituent in the 2-position. Early reports have claimed that ITP is not a substrate for EcRibA;[1] however, here we show that ITP is an exceptionally slow substrate and forms the DARP analogue 5-amino-6-$\beta$-pyrimidinone 5′-phosphate (ARP) in 50% of turnovers with the balance yielding IMP (Figure S5). Figure 7A depicts the net single-turnover data for EcRibA reacting with both GTP and ITP. These data indicate that ITP is converted to ARP (as observed at 310 nm) at a rate ~175-fold slower than GTP is converted to DARP. Moreover, the data obtained at 252 nm, which report predominantly binding/conformational activation and relaxation, were best fit to three exponential phases. Though there is no convenient way to measure the EcRibA·ITP binding constant, it is apparent that the binding of ITP is weak relative to GTP and that the rate of conformational activation observed is sevenfold slower than that observed with GTP at the same concentrations (0.36 vs 0.053 $s^{-1}$).

As with GTP and PPi, the ITP data do not fit to yield intrinsic rate constants but are delineated into three events

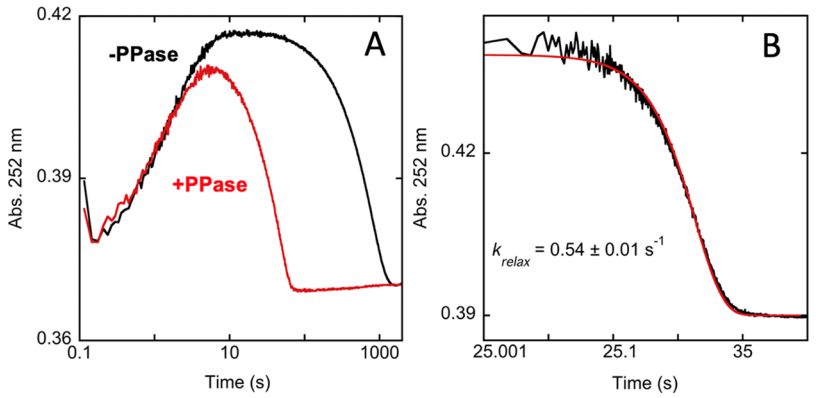


**Figure 6.** Effect of PPase on the relaxation of RibA in turnover with PPi. (A) RibA (100 $\mu$M) was mixed with PPi (25 $\mu$M), aged for 0.1 s, and then mixed with buffer (black trace) or trace pyrophosphatase (red trace). (B) RibA (100 $\mu$M) was mixed with PPi (25 $\mu$M), aged for 25 s, and then mixed with pyrophosphatase (1 $\mu$M) (black trace). The data were fit to a single-exponential expression (eq 1) to obtain the rate constant indicated.


https://doi.org/10.1021/acs.biochem.1c00511
Biochemistry 2021, 60, 3027−3039

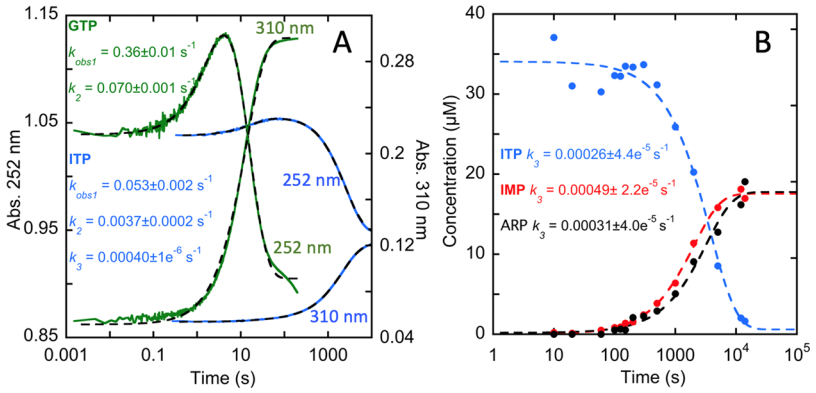


**Figure 7.** Transient-state single-turnover analysis of RibA in turnover with ITP. (A) Comparison of the kinetics observed with GTP (green) and ITP (blue). For each, 100 $\mu$M EcRibA was reacted with 40 $\mu$M nucleotide triphosphate and observed at 252 nm and at 310 nm for the DARP and ARP products. The GTP trace at 252 nm was fit to eq 1 for two exponentials, and the 310 nm trace was fit to eq 1 for one; the rate constants returned for the 252 nm data are indicated in green. The ITP trace at 252 was fit to eq 1 for three exponentials, and the 310 nm trace was fit to eq 1 for two; the rate constants returned for the 252 nm data are indicated in blue. (B) Acid quench product analysis of the reaction of 100 $\mu$M EcRibA with 40 $\mu$M ITP. Each trace was fit to one exponential according to eq 1.

**Scheme 2. Chemistry of RibA**

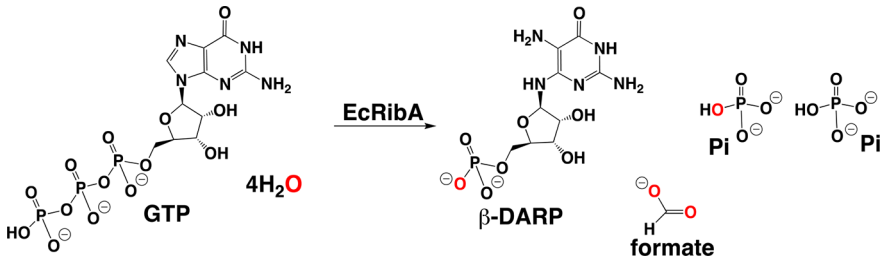


suggesting a fractional binding of ITP results in an intervening period where multiple turnovers occur with the small fraction of EcRibA that has ITP bound. Acid quench and product analysis were used both to confirm the reaction stoichiometry and to verify that no additional intermediate state accumulates in the net single-turnover reaction of EcRibA with ITP (Figure 7B). Control data show no significant hydrolysis of ITP by TCA to form IMP within the reaction times assessed. The data track only the loss of ITP and the accumulation of ARP and IMP coincident with the third phase observed. As such it is reasonable to conclude that the second phase observed does not indicate the accumulation of an additional intermediate species. Importantly, the summation of all species indicates that at no stage is there a deficit, revealing that none of the observed processes result in the formation of a stable covalent complex as has been frequently proposed to occur in the initial steps of the RibA catalytic cycle.[2,3,5,6,10] These results show that the decay of substrate and the accumulation of products closely matches that observed previously for GTP.[6] The slow but similar kinetics to those observed with GTP prompted the observation of the reaction using time-dependent $^{31}$P NMR (Figure S4). The spectra obtained over 550 min were combined into a single data set and were described by the model depicted in Figure S4B using a singular value decomposition. This model was derived from observations made with GTP and PPi as substrates and includes the opportunity for PPi to dissociate following the production of IMP and ARP. The time resolution available in this experiment is insufficient to constrain the kinetic values returned in fitting. As such the data were fit by fixing all the equilibrium and rate constants as indicated in Figure S4B with the exception of the binding constant for PPi and the rate of hydrolysis of PPi. The rate constants for the production of ARP and IMP were defined from the rate of the third phase observed for ITP in Figure 7A. The model does not include steps for enzyme activation, as these data do not report on this process in that the first spectrum was acquired ∼11 min after the reaction was initiated and does not capture data for the activation phase (Figure 7A). The deconvoluted spectra returned were composite and consistent with the succession of states; each spectrum represented multiple species that form and decay concomitantly. Importantly, the spectra reconstructed from the SVD analysis summarize the observation faithfully. While this process did not yield a reliable fit to the model shown, it does offer a descriptive account of what occurs with the ITP substrate. As indicated in Figure S4A, PPi accumulates with IMP and ARP; the PPi is then consumed on a longer time frame, indicating that it is freely dissociating during the production of ARP and IMP and hydrolyzed in an apparent steady state that is independent of the initial products. This differs from the GTP reaction in which the majority of the PPi is hydrolyzed during the production of DARP (Figures 4 & 5). The reason for this difference is possibly that the GTP reaction is committed forward such that the intermediate PPi does not dissociate. Required hydrolysis reactions at the purine therefore occur with PPi bound and before the PPi hydrolysis brings about a conformational relaxation. ITP is therefore uncoupled by ∼50% for the ARP formation and ∼100% for the Pi production.


https://doi.org/10.1021/acs.biochem.1c00511
Biochemistry 2021, 60, 3027−3039

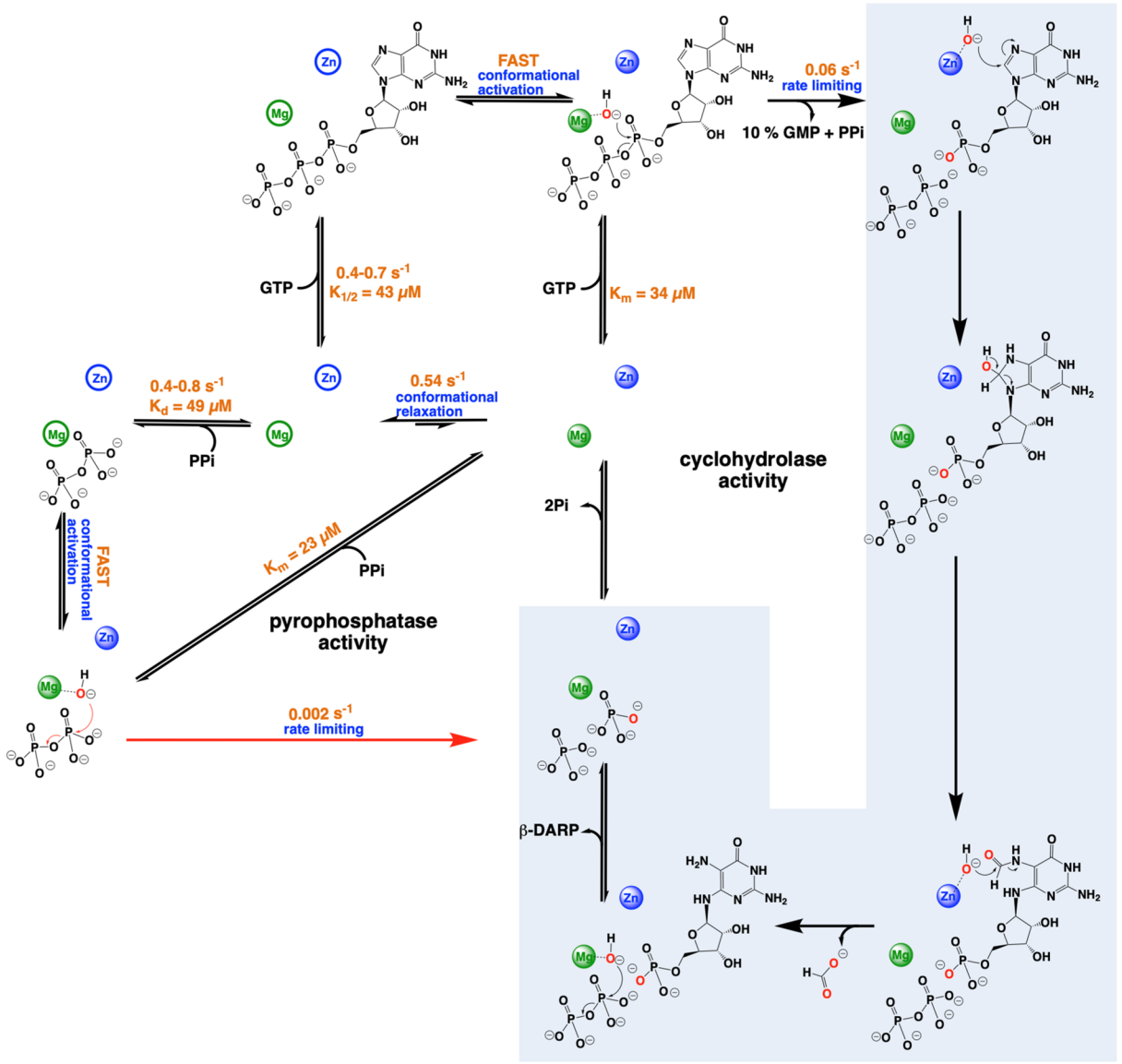


**Figure 8.** Summation of mechansitic conclusions. Metal ions depicted in unfilled circles represent nonactivated states. Metal ions depicted as spheres represent activated states. Measured parameters are shown in orange. Segments rendered with a blue background were inferred, as the data obtained does not report on these steps.

## CONCLUSIVE REMARKS

In 1975, Foor and Brown identified the second GTP cyclohydrolase activity from *E. coli*.[1] Using radiolabeled GTP, their work defined the stoichiometry of the GTP cyclohydrolase II reaction as producing formate, a pyrimidine nucleotide, and PPi as products. Since this study the stoichiometry of the RibA reaction has not been revisited other than a confirmatory observation of the accumulation PPi using $^{31}$P NMR.[5] It is a curious progression that, in the chronological sequence of GTP cyclohydrolase activity discoveries, the first did not alter the triphosphate moiety, the second was reported to cleave only at the $\alpha-\beta$ linkage yielding PPi,[1] and that the third cleaved both at the $\alpha-\beta$ and at the $\beta-\gamma$ linkages producing two Pi ions.[9] Here we present our findings from transient-state kinetic and product analyses that reveal a more complete description of the chemistry catalyzed by RibA.

Our data show that the binding of substrate GTP induces a rapid conformational change that is required to initiate four hydrolytic steps producing DARP, formate, and two Pi ions as products (Scheme 2). This stoichiometry though is not absolute, as some fraction of the PPi formed dissociates and is ultimately bound and hydrolyzed in a separate slow EcRibA PPase activity. This fraction is likely to be produced in a known abortive pathway that produces GMP as a product (Figure 8).[6] We conclude that the occupancy of the $\beta$ and $\gamma$ phospho-group binding sites stimulates EcRibA to change the conformation to a state that promotes hydrolytic reactions both at the magnesium and zinc metal ions. Figure 8 depicts the proposed chemistry of EcRibA based on our observations. In this figure it is proposed that there is no propensity for PPi to dissociate in the native cyclohydrolase activity but that it is released and rebound prior to a hydrolysis in the slow PPase activity. Our data suggest that, once the enzyme is conformationally activated in response to binding GTP, the hydrolysis of the $\alpha-\beta$ phosphodiester bond is the instigating and rate-limiting step in the EcRibA reaction accounting for the lack of accumulated catalytic intermediates. As such we theorize that,


https://doi.org/10.1021/acs.biochem.1c00511
Biochemistry 2021, 60, 3027−3039

for the majority of turnovers, the zinc hydrolytic chemistry at the purine is bookended by the magnesium-catalyzed hydrolytic processes at the phosphodiester bonds. However, the data shown does not conclusively support this, nor does it reveal the order of release of products. It is reasonable to surmise that DARP is bound when PPi is cleaved, as this chemistry occurs more rapidly than is observed with PPi alone. As such the cyclohydrolase and PPase catalytic cycles of RibA are cojoined at the point DARP is released from the enzyme.

In Figure 6 we show that the tendency of PPi to dissociate does not result in a rapid enzymatic relaxation, indicating that this substrate can be released and rebound to the activated state of EcRibA. A rapid relaxation was only possible with the hydrolysis of PPi by an external PPase enzyme. We therefore conclude that PPi can serve to sustain the enzyme in the conformationally activated state. Endogenous PPi is therefore a loosely bound substrate that does not significantly impede the association of GTP to the activated state for ensuing turnovers without an intervening reactivation step. In contrast, PPi does not dissociate from the EcRibA GTP reaction and conceivably functions in the intermediate state(s) to maintain the activated conformation, while the zinc hydrolytic chemistry cleaves formate from the guanine imidazole ring of GMP. These conclusions are made under the assumption that the relaxation is considerably slower than the GTP association/conformational activation. Additional evidence is that the $K_d$ for PPi is threefold lower than the $K_{1/2}$ measured for the binding of PPi to the resting enzyme (Figures 3B & S3), suggesting that the activated state is maintained in the steady state by PPi. Moreover, measured intracellular *E. coli* PPi concentrations approximate 500 $\mu$M, sufficient to maintain the activated state of EcRibA (Figure 3B).[20] This raises the possibility that the nonactivated state observed here is fundamentally an artifact of purification that is not a dominant form in the background of millimolar magnesium[21] and PPi in the cell. Certainly, stable concentrations of these reaction components would negate an evolutionary selection against such a state. Qualitative support for this hypothesis is obtained from comparison of the data shown in Figures 3B and 4B. In Figure 4B we observe that Pi is predominantly evolved during a conformation relaxation. In Figure 3B we observe that concentrations of PPi above 128 $\mu$M produce a distinctly square activation envelope indicative of there being a threshold PPi concentration that can balance dissociation and hydrolytic catalysis that prolongs the RibA activated state.

## ■ ASSOCIATED CONTENT

### Supporting Information

The Supporting Information is available free of charge at https://pubs.acs.org/doi/10.1021/acs.biochem.1c00511.

Control reaction demonstrating the effect of EDTA. Pseudo-first-order kinetics of phase one for EcRibA reacting with PPi. Competitive inhibition analysis of PPi versus GTP. Net single turnover of ITP monitored by $^{31}$P NMR. LCMS confirmation of the product of the RibA−ITP reaction (PDF)

## ■ AUTHOR INFORMATION


### Corresponding Author

**Graham R. Moran** − *Department of Chemistry and Biochemistry, Loyola University Chicago, Chicago, Illinois 60660, United States;* orcid.org/0000-0002-6807-1302; Phone: (773)508-3756; Email: gmoran3@luc.edu

### Authors

**Madison M. Smith** − *Department of Chemistry and Biochemistry, Loyola University Chicago, Chicago, Illinois 60660, United States*

**Brett A. Beaupre** − *Department of Chemistry and Biochemistry, Loyola University Chicago, Chicago, Illinois 60660, United States*

**Dariush C. Fourozesh** − *Department of Chemistry and Biochemistry, Loyola University Chicago, Chicago, Illinois 60660, United States*

**Kathleen M. Meneely** − *Department of Chemistry, University of Texas San Antonio, San Antonio, Texas 78249, United States*

**Audrey L. Lamb** − *Department of Chemistry, University of Texas San Antonio, San Antonio, Texas 78249, United States;* orcid.org/0000-0002-2352-2130

Complete contact information is available at: https://pubs.acs.org/10.1021/acs.biochem.1c00511


### Notes

The authors declare no competing financial interest.

Uniprot Identifiers. *Escherichia coli* RibA−B1LH12. *Escherichia coli* PNP−Q0T8S9. *Saccharomyces cerevisiae* PPase−P28239.

## ■ ACKNOWLEDGMENTS

This research was supported by Loyola University College of Arts and Sciences and National Science Foundation Grant Nos. 1904480 to G.R.M. and 1904494 to A.L.L. The authors express thanks to the NMR Facility Manager at Northwestern University Chemistry Department, Dr. Y. Zhang, for his assistance with $^{31}$P NMR measurements. The authors are also indebted to Dr. M. P. Chiarelli and his graduate student X. Martinez for the determination of the mass of the product of the RibA-ITP reaction.

## ■ REFERENCES


(1) Foor, F.; Brown, G. M. Purification and properties of guanosine triphosphate cyclohydrolase II from Escherichia coli. *J. Biol. Chem.* **1975**, *250*, 3545−3551.

(2) Lehmann, M.; Degen, S.; Hohmann, H. P.; Wyss, M.; Bacher, A.; Schramek, N. Biosynthesis of riboflavin. Screening for an improved GTP cyclohydrolase II mutant. *FEBS J.* **2009**, *276*, 4119−4129.

(3) Ren, J.; Kotaka, M.; Lockyer, M.; Lamb, H. K.; Hawkins, A. R.; Stammers, D. K. GTP cyclohydrolase II structure and mechanism. *J. Biol. Chem.* **2005**, *280*, 36912−36919.

(4) Richter, G.; Ritz, H.; Katzenmeier, G.; Volk, R.; Kohnle, A.; Lottspeich, F.; Allendorf, D.; Bacher, A. Biosynthesis of riboflavin: cloning, sequencing, mapping, and expression of the gene coding for GTP cyclohydrolase II in Escherichia coli. *J. Bacteriol.* **1993**, *175*, 4045−4051.

(5) Ritz, H.; Schramek, N.; Bracher, A.; Herz, S.; Eisenreich, W.; Richter, G.; Bacher, A. Biosynthesis of riboflavin: studies on the mechanism of GTP cyclohydrolase II. *J. Biol. Chem.* **2001**, *276*, 22273−22277.

(6) Schramek, N.; Bracher, A.; Bacher, A. Biosynthesis of riboflavin. Single turnover kinetic analysis of GTP cyclohydrolase II. *J. Biol. Chem.* **2001**, *276*, 44157−44162.

(7) Spoonamore, J. E.; Dahlgran, A. L.; Jacobsen, N. E.; Bandarian, V. Evolution of new function in the GTP cyclohydrolase II proteins of Streptomyces coelicolor. *Biochemistry* **2006**, *45*, 12144−12155.

(8) Burg, A. W.; Brown, G. M. The biosynthesis of folic acid. VI. Enzymatic conversion of carbon atom 8 of guanosine triphosphate to formic acid. *Biochim. Biophys. Acta, Gen. Subj.* **1966**, *117*, 275−278.
(9) Graham, D. E.; Xu, H.; White, R. H. A member of a new class of GTP cyclohydrolases produces formylaminopyrimidine nucleotide monophosphates. *Biochemistry* **2002**, *41*, 15074−15084.
(10) Kaiser, J.; Schramek, N.; Eberhardt, S.; Puttmer, S.; Schuster, M.; Bacher, A. Biosynthesis of vitamin B2. *Eur. J. Biochem.* **2002**, *269*, 5264−5270.
(11) Bracher, A.; Schramek, N.; Bacher, A. Biosynthesis of pteridines. Stopped-flow kinetic analysis of GTP cyclohydrolase I. *Biochemistry* **2001**, *40*, 7896−7902.
(12) Webb, M. R. A continuous spectrophotometric assay for inorganic phosphate and for measuring phosphate release kinetics in biological systems. *Proc. Natl. Acad. Sci. U. S. A.* **1992**, *89*, 4884−4887.
(13) Pace, N. C.; Vajdos, F.; Fee, L.; Grimsley, G.; Gray, T. How to measure and predict the molar absorption coefficient of a protein. *Protein Sci.* **1995**, *4*, 2411−2423.
(14) Johnson, K. A.; Simpson, Z. B.; Blom, T. Global kinetic explorer: a new computer program for dynamic simulation and fitting of kinetic data. *Anal. Biochem.* **2009**, *387*, 20−29.
(15) Johnson, K. A.; Simpson, Z. B.; Blom, T. FitSpace explorer: an algorithm to evaluate multidimensional parameter space in fitting kinetic data. *Anal. Biochem.* **2009**, *387*, 30−41.
(16) Zyryanov, A. B.; Shestakov, A. S.; Lahti, R.; Baykov, A. A. Mechanism by which metal cofactors control substrate specificity in pyrophosphatase. *Biochem. J.* **2002**, *367*, 901−906.
(17) Yadav, S.; Karthikeyan, S. Structural and biochemical characterization of GTP cyclohydrolase II from Helicobacter pylori reveals its redox dependent catalytic activity. *J. Struct. Biol.* **2015**, *192*, 100−115.
(18) Stockbridge, R. B.; Wolfenden, R. Enhancement of the rate of pyrophosphate hydrolysis by nonenzymatic catalysts and by inorganic pyrophosphatase. *J. Biol. Chem.* **2011**, *286*, 18538−18546.
(19) Schauble, S.; Stavrum, A. K.; Puntervoll, P.; Schuster, S.; Heiland, I. Effect of substrate competition in kinetic models of metabolic networks. *FEBS Lett.* **2013**, *587*, 2818−2824.
(20) Kukko, E.; Heinonen, J. The intracellular concentration of pyrophosphate in the batch culture of Escherichia coli. *Eur. J. Biochem.* **1982**, *127*, 347−349.
(21) Grubbs, R. D. Intracellular magnesium and magnesium buffering. *BioMetals* **2002**, *15*, 251−259.


https://doi.org/10.1021/acs.biochem.1c00511
*Biochemistry* 2021, 60, 3027−3039